

# Enhanced critical current density of *in situ* processed MgB<sub>2</sub> bulk superconductors with MgB<sub>4</sub> additions

S. H. Kim<sup>a,b</sup>, W. N. Kang<sup>b</sup>, B.-H. Jun<sup>a</sup>, Y. J. Lee<sup>a,b</sup>, and C.-J. Kim<sup>\*,a</sup>

<sup>a</sup>Korea Atomic Energy Research Institute, Daejeon, Korea

<sup>b</sup>Sungkyunkwan University, Suwon, Korea

(Received 25 January 2017; revised or reviewed 22 February 2017; accepted 23 February 2017)

## Abstract

The effects of MgB<sub>4</sub> addition on the superconducting properties and the microstructure of *in situ* processed MgB<sub>2</sub> bulk superconductors were studied. MgB<sub>4</sub> powder of 1-20 wt.% was mixed with (Mg + 2B) powder and then pressed into pellets. The pellets of (Mg + 2B + xMgB<sub>4</sub>) were heat-treated at 650 °C for 1 h in flowing argon. The powder X-ray diffraction (XRD) analysis for the heat-treated samples showed that the major formed phase in all samples was MgB<sub>2</sub> and the minor phases were MgB<sub>4</sub> and MgO. The full width at half maximum (FWHM) values showed that the grain size of MgB<sub>2</sub> decreased as the amount of MgB<sub>4</sub> addition increased. MgB<sub>4</sub> particles included in a MgB<sub>2</sub> matrix is considered to suppress the grain growth of MgB<sub>2</sub>. The onset temperatures ( $T_{c,onset}$ ) of MgB<sub>2</sub> with MgB<sub>4</sub> addition (0-10 wt.%) was between 37-38 K. The 20 wt.% MgB<sub>4</sub> addition slightly reduced the  $T_{c,onset}$  of MgB<sub>2</sub> to 36.5 K. This result indicates that MgB<sub>4</sub> addition did not influence the superconducting transition temperature ( $T_c$ ) of MgB<sub>2</sub> significantly. On the other hand, the small additions of 1-5 wt.% MgB<sub>4</sub> increased the critical current density ( $J_c$ ) of MgB<sub>2</sub>. The  $J_c$  enhancement by MgB<sub>4</sub> addition is attributed not only to the grain size refinement but also to the possible flux pinning of MgB<sub>4</sub> particles dispersed in a MgB<sub>2</sub> matrix.

**Keywords** : MgB<sub>2</sub>, MgB<sub>4</sub> addition, Superconductor, Critical current density ( $J_c$ ), Grain refinement

## 1. INTRODUCTION

A MgB<sub>2</sub> superconductor has a high superconducting critical temperature ( $T_c$ ) of 39 K [1] and a high critical current density ( $J_c$ ) at magnetic fields [2]. In addition to the excellent superconducting properties, other merits of MgB<sub>2</sub> are its long coherent length [3] and the small current anisotropy [4-5]. Moreover, the raw materials (Mg and B) of MgB<sub>2</sub> are not expensive and easy to obtain. Owing to these merits, MgB<sub>2</sub> is believed to be a promising material that can replace a conventional NbTi superconductor. A superconducting magnetic designed using MgB<sub>2</sub> superconducting wires can be operated at 20 K using an electrical cooler instead of liquid helium.

For practical applications of a MgB<sub>2</sub> superconductor the  $J_c$  under magnetic fields should be enhanced. The presence of defects in superconducting grains or at the grain boundaries of MgB<sub>2</sub> leads to the  $J_c$  enhancement of MgB<sub>2</sub>. The defects can be made artificially either through physical [6-13] or chemical [14-16] methods. Particle (neutron, electron or ion) irradiation is a well-known process that can form defects physically through the collision of accelerated particles to the targeting materials. Small defects such as vacancies and cavities can be formed in the superconducting matrix through particle irradiation [15-20]. As a result of the defect formation, the  $J_c$  at

the magnetic fields of the particle-irradiated MgB<sub>2</sub> was much higher than that of MgB<sub>2</sub> with no irradiation [21,22]. Along with the physical method, the  $J_c$  of MgB<sub>2</sub> can be increased by the doping of chemical species such as silicon carbide [23], carbon-related materials [24], and other fine impurity phases [25]. The carbon doping to MgB<sub>2</sub> not only led to the formation of a lattice strain [26], and lattice substitution [26-31] but also increased the number of grain boundaries [32]. Mechanical milling for boron powder is an alternative way to increase the  $J_c$  of MgB<sub>2</sub> through the grain size refinement of MgB<sub>2</sub> [32].

In this experiment, MgB<sub>4</sub> powder was synthesized using Mg and B powder by the powder reaction process. MgB<sub>4</sub> is a phase that is compatible with MgB<sub>2</sub> in a Mg-B binary phase diagram. MgB<sub>4</sub> is often formed with MgB<sub>2</sub> in the powder reaction process using boron-enriched compositions. The synthesized MgB<sub>4</sub> powder was used as an additive of *in situ* processed MgB<sub>2</sub> bulk superconductors. The added amount of MgB<sub>4</sub> was changed from 0 to 20 wt.%. The effects of MgB<sub>4</sub> addition on the  $J_c$ ,  $T_c$  and the microstructure of MgB<sub>2</sub> were investigated.

## 2. EXPERIMENTAL PROCEDURE

MgB<sub>4</sub> powder used as an additive for MgB<sub>2</sub> superconductors was synthesized by the powder reaction method of (Mg + 4B = MgB<sub>4</sub>) using Mg and B powders.

\* Corresponding author: [cjkim2@kaeri.re.kr](mailto:cjkim2@kaeri.re.kr)

The detailed preparation condition of  $MgB_4$  was well described in previous reports [33-38]. The impurity phases included in the synthesized  $MgB_4$  powder were removed by the  $HNO_3$  leaching process [36].

$MgB_2$  bulk superconductors were fabricated through an *in situ* reaction process using Mg and B powders. Mg and B powders with a ratio of Mg:B=1:2 were mixed for 30 min by hand mixing using a mortar jar and pestle. To compensate the possible Mg loss during heat treatment, 10 wt.% of Mg was intentionally added to a mixture of (Mg + 2B).  $MgB_4$  powder of 1-20 wt.% was added to the mixture of (Mg + 2B) powder.

0.3 g of a powder mixture of (Mg + 2B + x wt.%  $MgB_4$ ) was put in a steel mold with a diameter of 10 mm and was uniaxially pressed into a pellet. The pressed pellet was encapsulated with a Ti tube to suppress the possible oxidation of Mg during heat treatment. To determine out the optimum heat treatment condition for the formation of  $MgB_2$ , the heat treatment temperature and time were varied. We determined the heat treatment temperature as  $650^\circ C$ , which is a temperature just above a melting point of Mg and the heat treatment period as 1 h. The short period of 1 h at  $650^\circ C$  is to minimize the grain growth of  $MgB_2$ . The Ti-encapsulated pellets were located at the center of a tubular furnace, heated to  $650^\circ C$  at a rate of  $100^\circ C/h$  in flowing argon gas, maintained for 1 h and then cooled to room temperature in a furnace.

The heat treated pellets were crushed into a powder form for a phase analysis. The formed phases after heat treatment were analyzed using an X-ray diffraction method (XRD) for the power samples. From the peak intensity of each phase in XRD patterns, volume fractions of the formed phases and the second residual phases were calculated using eq. (1).

$$F(MgB_2) = \frac{\sum I_{MgB_2}}{\sum I_{MgB_2} + \sum I_{MgB_4} + \sum I_{MgO}} \quad (1)$$

where  $F(MgB_2)$  is a volume fraction of  $MgB_2$ , and  $I_{MgB_2}$  and  $I_{MgB_4}$  and  $I_{MgO}$  are the peak intensities of  $MgB_2$ ,  $MgB_4$  and  $MgO$ , respectively.

To measure  $T_c$  and  $J_c$  of  $MgB_2$  bulk superconductors, rectangular specimens with approximate dimensions of  $3 \times 3 \times 2$  mm were cut from the heat-treated pellets using a diamond saw. Susceptibility-temperature curves ( $M-T$ ) and magnetization-magnetic field ( $M-H$ ) curves are obtained using a magnetic properties measurement system (MPMS) with a maximum magnetic field of 5 Tesla.  $J_c$  at 5 K and 20 K was calculated using the extended Bean's critical model [39] of eq. (2).

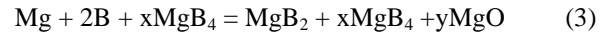
$$J_c = 20\Delta M/a(1-a/3b) \quad (2)$$

where  $\Delta M$  is the magnetization difference (M\_decreasing field region-M\_increasing field region) in a constant magnetic field, and  $a$  and  $b$  are parameters regarding the sample dimension.

### 3. RESULTS AND DISCUSSION

Fig. 1 shows the XRD patterns of the samples with (0-20 wt.%)  $MgB_4$  additions, heat-treated at  $650^\circ C$  for 1 h. The major formed phase of all samples is  $MgB_2$  regardless of the amount of  $MgB_4$  additions. The addition of  $MgB_4$  appears to not affect the formation of  $MgB_2$ . As the amount of  $MgB_4$  addition increases, the peaks of  $MgB_4$  are intensified (see the XRD patterns with 10 and 20 wt.%  $MgB_4$  additions). Another minor phase formed in the heat-treated pellets is  $MgO$ . Small  $MgO$  peaks observed in all XRD patterns are attributed to the oxidation of Mg during heat treatment.

According to the XRD results of Fig. 1, the formation reaction of  $MgB_4$  at the give heat treatment condition can be described by eq. (3).



At the heat treatment temperature of  $650^\circ C$ ,  $MgB_2$  forms through the liquid phase reaction between a Mg melt and a solid B powder, because the heat treatment temperature is high than m. p. ( $649^\circ C$ ) of Mg. The formation reaction of  $MgB_2$  would be conducted by the mass transfer through the Mg melt. Most of the Mg is thought to be consumed to form  $MgB_2$  through the reactions of ( $Mg + 2B = MgB_2$ ) and ( $MgB_4 + Mg = MgB_2$ ). Some of the Mg might be consumed for the oxidation of Mg or be evaporated during heat treatment. Because 10 wt.% of Mg was intentionally added to the raw powders of (Mg + B) to compensate the Mg loss, the amount of Mg was sufficient for the formation reaction of  $MgB_2$ . In the case of large  $MgB_4$  additions, The peaks of  $MgB_4$  were present together with  $MgB_2$ . The  $MgB_4$  is supposed to be present as a discrete particle form within  $MgB_2$  grains or at the grain boundaries of  $MgB_2$ .

Fig. 2 shows the volume fraction of the formed phases in the samples with  $MgB_4$  additions, calculated using eq. (1).

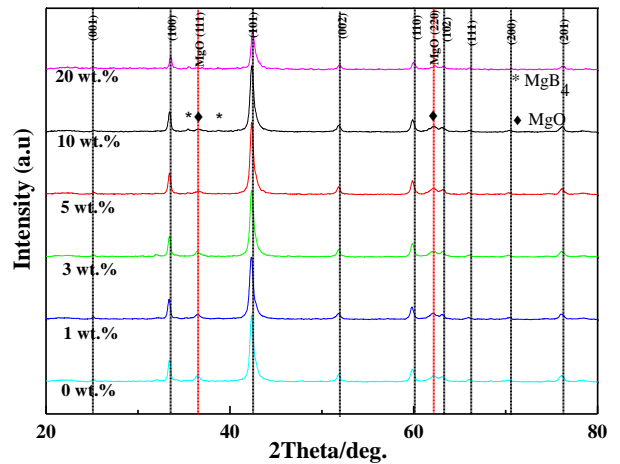


Fig. 1. XRD patterns of the samples with  $MgB_4$  additions, heat-treated at  $650^\circ C$  for 1 h.

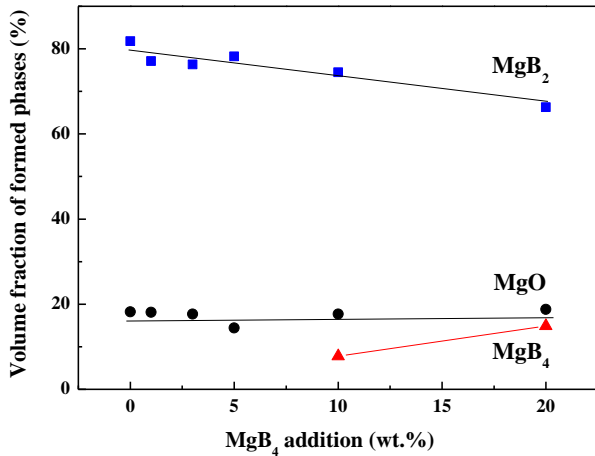


Fig. 2. Volume fractions of MgB<sub>2</sub>, MgB<sub>4</sub> and MgO as a function of the amount of MgB<sub>4</sub> addition.

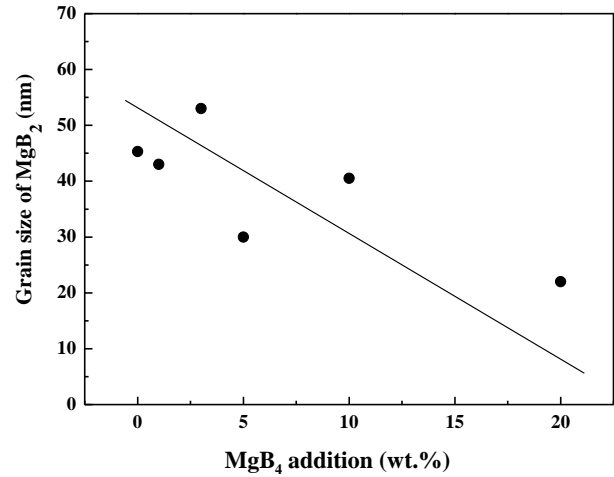


Fig. 3. Variation of grain size of MgB<sub>2</sub> as a function of the amount of MgB<sub>4</sub> addition.

TABLE I  
LATTICE PARAMETERS AND FWHM VS. AMOUNT OF MgB<sub>4</sub> ADDITION.

Amount of MgB <sub>4</sub> (wt.%)	FWHM (deg.)		Lattice parameter (Å)	
	(110)	(002)	a	c
0	0.389	0.443	3.090	3.532
1	0.415	0.449	3.091	3.500
3	0.405	0.413	3.087	3.534
5	0.391	0.425	3.088	3.540
10	0.403	0.455	3.090	3.526
20	0.396	0.486	3.087	3.497

The volume fraction of MgB<sub>2</sub> of the sample with no addition is approximately 80%. As is normally expected, the volume fraction of MgB<sub>2</sub> is dependent on the added amount of MgB<sub>4</sub>. The volume fractions of MgB<sub>2</sub> for the sample with 10 wt.% and 20 wt.% MgB<sub>4</sub> additions are 74% and 66.3%, respectively. Interestingly, the volume fraction of the MgO formed during heat treatment is approximately 18% regardless of the MgB<sub>4</sub> addition.

Through a precise analysis of the XRD patterns of Fig. 1, the lattice parameters of MgB<sub>2</sub> and the full width at half maximum (FWHM) of the peaks were calculated, the results of which are summarized in TABLE I. As illustrated in TABLE I, the lattice parameters *a* and *c* were not influenced by the MgB<sub>4</sub> additions. This is because both MgB<sub>2</sub> and MgB<sub>4</sub> are stoichiometric line compounds and there is no interaction between MgB<sub>2</sub> and MgB<sub>4</sub> (MgB<sub>4</sub> is a high temperature phase). The values of FWHM estimated from the (110) and (002) peaks of MgB<sub>2</sub> increase as the amount of MgB<sub>4</sub> addition increases, which indicates the change in the grain size of MgB<sub>2</sub>.

The grain sizes of MgB<sub>2</sub> samples with no addition and MgB<sub>4</sub> additions were calculated from the formula  $t = 0.9\lambda / B \cos\theta$  [40] using the FWHM data. Where *t* is the grain (crystallite) size,  $\lambda$  is the wavelength of the target used, *B* is the half width of the peak, and  $\theta$  is the Bragg angle of the incident beam.

Fig. 3 shows the variation of the grain size of MgB<sub>2</sub> as a function of the amount of MgB<sub>4</sub> addition. The grain size of

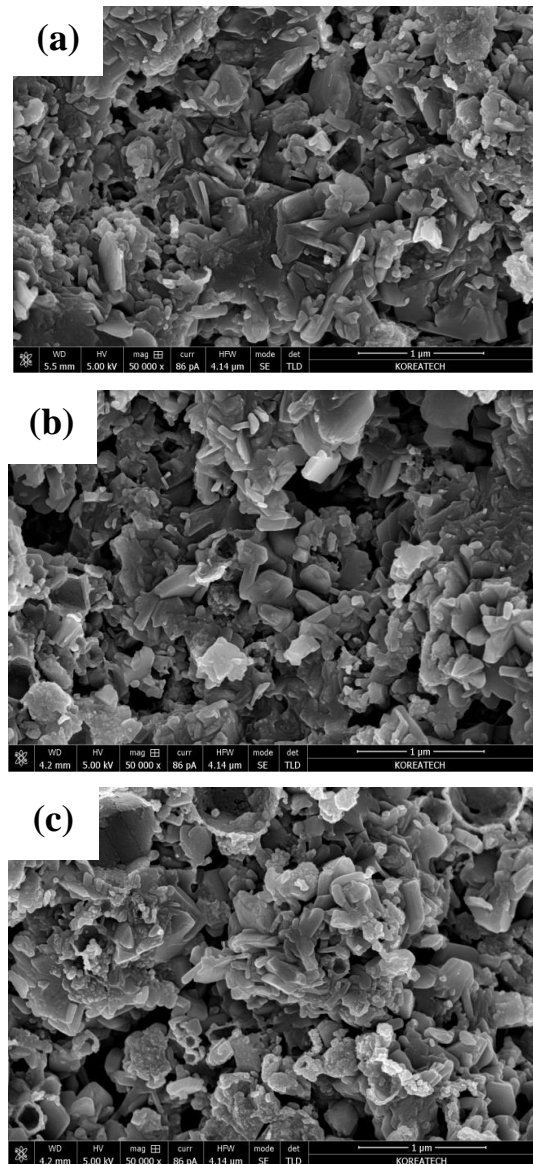


Fig. 4. SEM micrographs of samples with (a) no addition, (b) 5 wt.% MgB<sub>4</sub> addition, and (c) 20 wt.% MgB<sub>4</sub> addition.

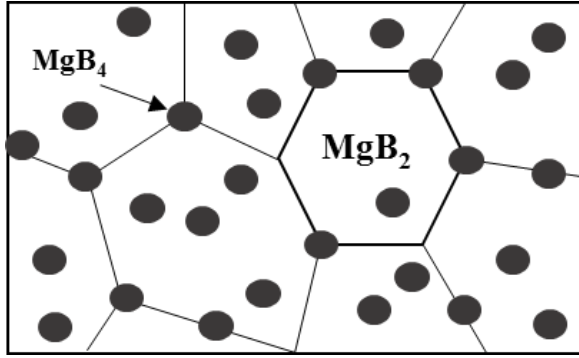


Fig. 5. Schematics of dispersed  $\text{MgB}_4$  particles in an  $\text{MgB}_2$  grain structure.

$\text{MgB}_2$  with no addition is 45 nm. The grain size decreases as the amount of  $\text{MgB}_4$  addition increases. For 5 wt.% and 20 wt.%  $\text{MgB}_4$  additions, the grain sizes of  $\text{MgB}_2$  are 30 nm and 22 nm, respectively. These results indicate that the  $\text{MgB}_4$  addition suppressed the grain growth of  $\text{MgB}_2$ . In other words, a larger grain boundary area exists in the pellet with  $\text{MgB}_4$  addition in comparison with no addition.

Fig. 4 shows SEM micrographs of the samples with (a) no addition, (b) 5 wt.%  $\text{MgB}_4$  addition and (c) 20 wt.%  $\text{MgB}_4$  addition. Many plate-like grains whose thickness is smaller than 1  $\mu\text{m}$  are observed in sample (a). As already confirmed through the XRD analysis of Fig. 1, approximately 80 % of the formed phase of sample (a) was  $\text{MgB}_2$ . It can thus be said that the plate-like grains are  $\text{MgB}_2$ . The SEM investigation showed that the grain size of  $\text{MgB}_2$  decreased as the amount of  $\text{MgB}_4$  addition increased. The  $\text{MgB}_2$  grains observed in the sample with 20 wt. %  $\text{MgB}_4$  addition are smaller than that of sample (a) (see Fig. 4c)). The SEM observation agrees with the XRD FWHM of Fig. 2.

The reason why the grain growth of  $\text{MgB}_2$  was suppressed by the addition of  $\text{MgB}_4$  can be explained in terms of the thermal stability of  $\text{MgB}_4$  at the heat treatment temperatures. There is a large difference in the melting temperature between Mg and B. The m. p. of B is as high as 2300 $^\circ\text{C}$  [41], whereas the m. p. of Mg is very low at 649 $^\circ\text{C}$  [42].  $\text{MgB}_4$ , which has more boron than  $\text{MgB}_2$ , would be more stable at high temperature. The  $\text{MgB}_4$  particles can be present at the grain boundaries of  $\text{MgB}_2$  or trapped within  $\text{MgB}_2$  grains (see the schematic illustration in Fig. 5). The  $\text{MgB}_4$  particle present at the grain boundaries of  $\text{MgB}_2$  can suppress the grain growth of  $\text{MgB}_2$  during heat treatment.

Fig. 6 shows normalized susceptibility-temperature ( $M-T$ ) curves of the samples with various  $\text{MgB}_4$  additions.  $T_{c,onset}$  and  $T_{c,mid}$  of the sample with no addition are 37 K and 35.9 K, respectively, whereas  $T_{c,onset}$  and  $T_{c,mid}$  of the sample with 10 wt.%  $\text{MgB}_4$  addition are 37 K and 36.1 K, respectively. In the case of a large  $\text{MgB}_4$  addition of 20 wt.%,  $T_{c,onset}$  and  $T_{c,mid}$  are 36.5 K and 35.8 K, which are slightly lower than the other samples. The superconducting critical temperatures seem to not be significantly influenced by the  $\text{MgB}_4$  addition. The  $M-T$  result confirms again that  $\text{MgB}_4$  is a chemically stable and thermally compatible additive with  $\text{MgB}_2$ , which does not react with

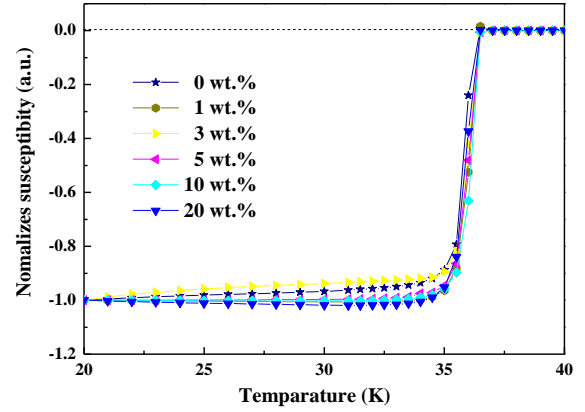


Fig. 6. Normalized susceptibility-temperature curves of the samples with  $\text{MgB}_4$  additions.

TABLE II  
SUPERCONDUCTING TRANSITION TEMPERATURES OF THE SAMPLES WITH  $\text{MgB}_4$  ADDITIONS.

$\text{MgB}_4$ addition (wt.%)	Superconducting critical temperatures of $\text{MgB}_2$ (K)	
	$T_{c,onset}$	$T_{c,mid}$
0	37	35.9
1	37	36.0
3	37.5	36.3
5	38	37.3
10	37	36.1
20	36.5	35.8

a superconducting  $\text{MgB}_2$ . The superconducting critical temperatures of the samples with various  $\text{MgB}_4$  additions are summarized in TABLE II.

Fig. 7 shows  $J_c-B$  curves at 5 K and 20 K of samples with  $\text{MgB}_4$  additions, heat-treated at 650 $^\circ\text{C}$  for 1 h. The  $J_s$  at 5 K of the samples with 1-5 wt.%  $\text{MgB}_4$  additions are slightly higher than that of the sample with no addition. Moreover,  $J_c$  at 5 K of the sample with 10 wt.%  $\text{MgB}_4$  is similar to that of the sample with no addition, in spite of the low volume fraction of  $\text{MgB}_2$ . The enhanced  $J_c$  of the samples with small  $\text{MgB}_4$  additions is attributed to the grain refinement and the presence of  $\text{MgB}_4$  particles in the superconducting  $\text{MgB}_2$  matrix, which were already observed by FWHM and SEM investigations (Figs. 3 and 4). These two factors appear to act as flux pinning centers which pin the magnetic flux. When the amount of  $\text{MgB}_4$  addition is more than 20 wt.%,  $J_c$  decreases because the superconducting volume fraction in the sample decreases. Although not shown here, in our study, the addition of  $\text{MgB}_4$  up to 70% resulted in a decrease in  $J_c$  in proportion to the amount added. The  $J_c-B$  characteristics at 20 K of samples with  $\text{MgB}_4$  additions shows similar trend to that at 5 K: 1-5 wt.%  $\text{MgB}_4$  additions increases the  $J_c$  of  $\text{MgB}_2$ .

Fig. 8 shows the  $J_c-B$  curves at 5 K and the magnetic fields of 3.5-5.0 T. With the exception of the 20 wt.%  $\text{MgB}_4$  addition, the  $J_c$  values at 5 K and the given applied magnetic fields of the samples are higher than that of the sample with no addition.  $J_c$  at 5 K, 4 T of the sample with no addition is 50,850 A/cm $^2$ , whereas  $J_c$ s at 5 K, 4 T of the samples with 1 wt.% and 3 wt.%  $\text{MgB}_4$  additions are 59,920 A/cm $^2$  and 60,760 A/cm $^2$ , respectively.



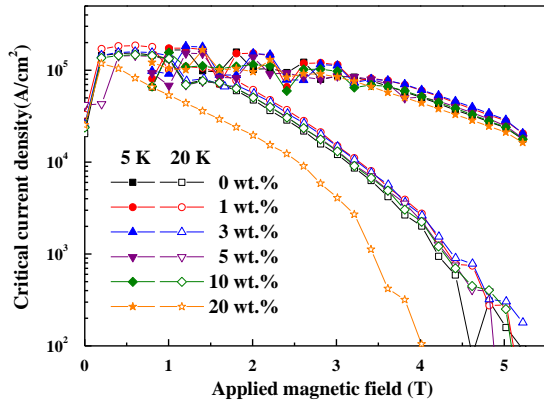


Fig. 7.  $J_c$ - $B$  curves at 5 K and 20 K of the samples with 0-20 wt.% MgB<sub>4</sub> additions.

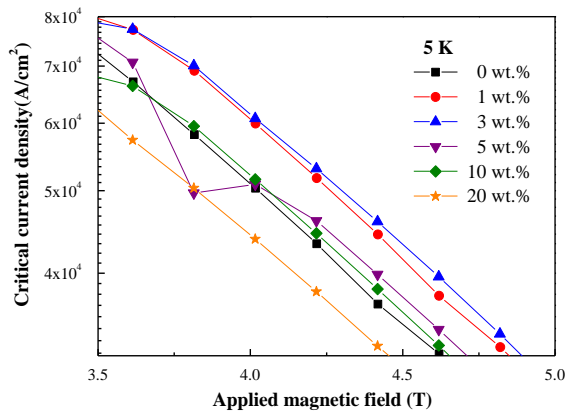


Fig. 8.  $J_c$ - $B$  curves at 5 K and magnetic fields of 3.5 T-5.0 T of the samples with 0-20 wt.% MgB<sub>4</sub> additions.

#### 4. CONCLUSIONS

We studied the effects of MgB<sub>4</sub> additions (1-20 wt.%) on the superconducting properties of MgB<sub>2</sub> bulk superconductors prepared using the powder reaction process. The onset temperature ( $T_{c,onset}$ ) of MgB<sub>2</sub> with MgB<sub>4</sub> addition (0-10 wt.%) was between 37-38 K. Even for a large MgB<sub>4</sub> addition of 20 wt.%, the  $T_{c,onset}$  was 36.5 K. This result indicates that the MgB<sub>4</sub> addition did not significantly influence the superconducting transition temperature ( $T_c$ ) of MgB<sub>2</sub>. On the other hand, the small MgB<sub>4</sub> additions of 1-5 wt.% increased the critical current density ( $J_c$ ) of MgB<sub>2</sub>. Moreover, the  $J_c$  level of MgB<sub>2</sub> with 10 wt.% MgB<sub>4</sub> addition was similar to that of MgB<sub>2</sub> with no addition in spite of the reduced superconducting volume. The FWHM and SEM investigation showed that the grain size of MgB<sub>2</sub> decreased as the amount of MgB<sub>4</sub> addition increased. The presence of MgB<sub>4</sub> in a MgB<sub>2</sub> matrix is likely to suppress the grain growth of MgB<sub>2</sub> at the heat treatment temperature. The  $J_c$  enhancement of MgB<sub>2</sub> by the MgB<sub>4</sub> addition appears to be attributed to the grain size refinement of MgB<sub>2</sub> and the possible flux pinning of MgB<sub>4</sub> particles dispersed within MgB<sub>2</sub> grains.

#### ACKNOWLEDGMENTS

This work was supported by the National Research Foundation Grant (NRF-2013M2A8A1035822) from Ministry of Science, ICT and Future Planning (MSIP) of Republic of Korea, and partially supported by Korea Institute for Advancement of Technology (KIAT) through the Promoting Regional specialized Industry.

#### REFERENCES

- [1] J. Nagamatsu, N. Nakagawa, T. Muranaka, Y. Zenitani and J. Akimitsu, "Superconductivity at 39 K in magnesium diboride," *Nature*, vol. 410, pp. 63-64, 2001.
- [2] Y. Eltsev, S. Lee, K. Nakao, N. Chikumoto, S. Tajima, N. Koshizuka and M. Murakami, "Anisotropic superconducting properties of MgB<sub>2</sub> single crystals probed by in-plane electrical transport measurements," *Phys. Rev.*, vol. 65, pp. 140501, 2002.
- [3] M. Eisterer, M. Zehetmayer and H. W. Weber, "Current percolation and anisotropy in polycrystalline MgB<sub>2</sub>," *Phys. Rev. Lett.*, vol. 90, pp. 247002, 2003.
- [4] Y. Eltsev, S. Lee, K. Nakao, N. Chikumoto, S. Tajima, N. Koshizuka and M. Murakami, "Anisotropic superconducting properties of MgB<sub>2</sub> single crystals probed by in-plane electrical transport measurements," *Phys. Rev.*, vol. 65, pp. 140501, 2002.
- [5] A. V. Pan, S. Zhou, H. Liu and S. Dou, "Properties of superconducting MgB<sub>2</sub> wires: *in situ* versus *ex situ* reaction technique," *Supercond. Sci. Technol.*, vol. 16, pp. 639-644, 2003.
- [6] Y. J. Zhao, W. K. Chu, M. F. Davis, J. C. Wolfe, S. C. Deshmukh and D. J. Economou, "Radiation damages and flux pinning in YBa<sub>2</sub>Cu<sub>3</sub>O<sub>7</sub> thin films," *Physica C*, vol. 184, pp. 144-148, 1991.
- [7] L. Gozzelino, D. Botta, R. Cherubini, A. Chiodoni, R. Gerbaldo, G. Ghigo and F. Laviano, "Proton irradiation induced effects on YBCO films analyzed by magneto-optics," in *Magneto-Optical Imaging*, vol. 142, T. H. Johansen and D. V. Shantsev, Eds. Springer Netherlands, 2004, pp. 197-204.
- [8] F. M. Sauerzopf, H. P. Wiesinger and H. W. Weber, "Analysis of pinning effects in YBa<sub>2</sub>Cu<sub>3</sub>O<sub>7- $\delta$</sub>  single crystals after fast neutron irradiation," *Phys. Rev. B*, vol. 51, pp. 6002-6012, 1995.
- [9] F. M. Sauerzopf, H. P. Wiesinger, H. W. Weber, G. W. Crabtree and J. Z. Liu, "Neutron-irradiation effects on critical current densities in single-crystalline YBa<sub>2</sub>Cu<sub>3</sub>O<sub>7- $\delta$</sub> ," *Phys. Rev. B*, vol. 43, pp. 3091-3100, 1991.
- [10] T. Kato, K. Shiraishi and J. Kuniya, "Enhanced critical magnetization currents due to electron irradiation in high- $T_c$  oxide superconductors," *Jpn. J. Appl. Phys.*, vol. 28, pp. 766-768, 1989.
- [11] M. A. Kirk and Y. Yan, "Structure and properties of irradiation defects in YBa<sub>2</sub>Cu<sub>3</sub>O<sub>7- $x$</sub> ," *Micron*, vol. 30, pp. 507-526, 1999.
- [12] H. Matsui, H. Ogiso, H. Yamasaki, M. Sohma, I. Yamaguchi, T. Kumagai, and T. Manabe, "Influence of middle-energy ion-irradiation on the flux pinning properties of YBCO films: Comparison between different synthesis methods," *J. Phys. Conf. Ser.*, vol. 507, pp. 022019, 2014.
- [13] N. M. Strickland, E. F. Talantsev, N. J. Long, J. A. Xia, S. D. Searle, J. Kennedy, A. Markwitz, M. W. Rupich, X. Li and S. Sathyamurthy, "Flux pinning by discontinuous columnar defects in 74 MeV Ag-irradiated YBa<sub>2</sub>Cu<sub>3</sub>O<sub>7</sub> coated conductors," *Physica C*, vol. 469, pp. 2060-2067, 2009.
- [14] G. Krabbes, G. Fuchs, P. Schatzle, S. Grup, J. W. Park, F. Hardinghaus, G. Stover, R. Hayn, S. L. Drechsler and T. Fahr, "Zn doping of YBa<sub>2</sub>Cu<sub>3</sub>O<sub>7</sub> in melt textured materials: peak effect and high trapped field," *Physica C*, vol. 330, pp. 181-190, 2000.
- [15] M. Daeumling, J. M. Seuntjens and D. C. Larbalestier, "Oxygen-defect flux pinning, anomalous magnetization and intra-grain granularity in YBa<sub>2</sub>Cu<sub>3</sub>O<sub>7- $\delta$</sub> ," *Nature*, vol. 346, pp. 332-335, 1990.
- [16] M. Mironova, D. F. Lee and K. Salama, "TEM and critical current density studies of melt-textured YBa<sub>2</sub>Cu<sub>3</sub>O<sub>x</sub> with silver and Y<sub>2</sub>BaCu<sub>3</sub>O<sub>5</sub> additions," *Physica C*, vol. 211, pp. 188-204, 1993.
- [17] A. Di'az, L. Mechin, P. Berghuis, and J. E. Evetts, "Evidence for vortex pinning by dislocations in YBa<sub>2</sub>Cu<sub>3</sub>O<sub>7- $\delta$</sub>  low-angle grain boundaries," *Phys. Rev. Lett.*, vol. 80, pp. 3855-3858, 1998.

- [18] H. Yamasaki, Y. Nakagawa, A. Sawa, H. Obara and K. Develos, "Flux pinning effects of twin boundaries studied with unidirectionally twinned YBCO films," *Physica C*, vol. 372-376, pp. 1885-1889, 2002.
- [19] Z. L. Wang, A. Goyal and D. M. Korger, "Structural and chemical disorder near the  $Y_2BaCuO_5/YBa_2CuO_{7-\delta}$  interface and its possible relation to the flux-pinning behavior in melt-textured  $YBa_2Cu_3O_{7-\delta}$ ," *Phys. Rev. B*, vol. 47, pp. 5773-5382, 1993.
- [20] C. J. Kim and G. W. Hong, "Defect formation, distribution and size reduction of  $Y_2BaCuO_5$  in melt-processed YBCO superconductors," *Supercond. Sci. Technol.*, vol. 12, pp. 24-41, 1999.
- [21] Tania M. Silver, J. Horvat, M. Reinhard, P. Yao, S. Keshavarzi, P. Munroe and S. X. Dou, "Uranium Doping and Thermal Neutron Irradiation Flux Pinning Effects in  $MgB_2$ ," *Appl. Supercond.*, vol. 14, pp. 33-39, 2004.
- [22] I. Pallecchi, C. Tarantini, H. U. Aebersold, V. Braccini, C. Fanciulli, C. Ferdeghini, F. Gatt, E. Lehmann, P. Manfrinetti, D. Marré, A. Palenzona, A. S. Siri, M. Vignolo and M. Putti, "Enhanced flux pinning in neutron irradiated  $MgB_2$ ," *Phys. Rev. B*, vol. 71, pp. 212507, 2005.
- [23] X. H. Zeng, A. V. Pogrebnikov, M. H. Zhu, J. E. Jones, X. X. Xi, S. Y. Xu, Wertz and Qi Li, "Superconducting  $MgB_2$  thin films on silicon carbide substrates by hybrid physical-chemical vapor deposition," *Appl. Phys. Letts.*, vol. 82, 13, 2003.
- [24] B. H. Jun and C. J. Kim, "The effect of heat-treatment temperature on the superconducting properties of malic acid-doped  $MgB_2/Fe$  wire," *Supercond. Sci. Technol.*, vol. 20, pp. 980-985, 2007.
- [25] Qi Cai, Yongchang Liu, Zongqing Ma and Zhizhong Dong, "Superconducting properties of  $Y_2O_3/SiC$  Co-doped bulk  $MgB_2$ ," *J Supercond.*, vol. 25, pp. 357-361, 2012.
- [26] A. Serquis, Y. T. Zhu, E. J. Peterson, J. Y. Coulter, D. E. Peterson, and F. M. Mueller, "Effect of lattice strain and defects on the superconductivity of  $MgB_2$ ," *Amer. Inst. Phys.*, vol. 79, pp. 4399-4401, 2001.
- [27] W. K. Yeoh and S. X. Dou, "Enhancement of  $H_{c2}$  and  $J_c$  by carbon-based chemical doping," *Physica C*, vol. 456, pp. 170-179, 2007.
- [28] R. H. T. Wilke, S. L. Bud'ko, P. C. Canfield and D. K. Finnemore, "Systematic Effects of Carbon Doping on the Superconducting Properties of  $Mg(B_{1-x}C_x)_2$ ," *Phys. Rev. Lett.*, vol. 92, 217003, 2004.
- [29] H. Yamada, M. Hirakawa, H. Kumakura and H. Kitaguchi, "Effect of aromatic hydrocarbon addition on *in situ* powder-in-tube processed  $MgB_2$  Tapes," *Supercond. Sci. Technol.* vol. 19, pp. 175-177, 2006.
- [30] Y.-J. Kim, B.-H. Jun, K.S. Tan, B.G. Kim, J.M. Sohn and C.-J. Kim, "Effect of glycerin addition on the superconducting properties of  $MgB_2$ ," *Physica C*, vol. 468, pp. 1372-1374, 2008.
- [31] K.S. Tan, S.K. Chen, B.-H. Jun and C.-J. Kim, "Enhancement in critical current density and irreversibility field of bulk  $MgB_2$  by C and  $CaCO_3$  co-addition," *Supercond. Sci. Technol.*, vol. 21, 105013, 2008.
- [32] B.-H. Jun, N.-K. Kim, K.S. Tan and C.-J. Kim, "Enhanced critical current properties of *in situ* processed  $MgB_2$  wires using milled boron powder and low temperature solid-state reaction," *J. Alloys Compd.*, vol. 492, pp. 446-451, 2010.
- [33] K. L. Tan, K. P. Lim, A. S. Halim and S. K. Chen, "Enhanced critical current density in  $MgB_2$  prepared by reaction of  $MgB_4$  and Mg," *Phys. Stat. Sol. A* 210, no. 3, pp. 616-622, 2013.
- [34] D Nardelli, D Matera, M Vignolo, G Bovone, A. Palenzona, A. S. Siri and G. Grasso, "Large critical current density in  $MgB_2$  wire using  $MgB_4$  as precursor," *Supercond. Sci. Technol.*, vol. 26, pp. 075010, 2013.
- [35] A. Ito, A. Yamamoto, J. Shimoyama, H. Ogino and K. Kishio "Synthesis of denser *in situ*  $MgB_2$  bulks using  $MgB_4$  precursor," *Appl. Supercond.*, vol. 23, pp. 7101005, 2013.
- [36] K. L. Tan, K. Y. Tan, K. P. Lim, S. A. Halim and S. K. Chen, "Synthesis of  $MgB_2$  from  $MgB_4$  through combinatorial solid state reaction routes," *Solid State Sci. and Technol.*, vol. 19, pp.15-19, 2011.
- [37] J. Ishiwata, M. Muralidhar, K. Inoue and M. Murakami, "Effect of  $MgB_4$  addition on the Superconducting Properties of Polycrystalline  $MgB_2$ ," *Physics Procedia*, vol.65, pp. 69-72, 2015.
- [38] K. S. Tan, B. H. Jun and C. J. Kim, "Superconducting Properties of a  $MgB_2$  Bulk Formed by Using a  $MgB_4 + Mg$  Mixture," *J. Korean Phys. Soc.*, vol. 54, no. 4, pp.1626-1629, 2009.
- [39] C. P. Bean, "Magnetization of High-Field Superconductors," *Rev. Mod. Phys.*, vol. 36, pp.31-39, 1964.
- [40] P. Scherrer, "Bestimmung der Größe und der inneren Struktur von Kolloidteilchen mittels Röntgenstrahlen," *Nachr. Ges. Wiss. Göttingen* 26, pp 98-100, 1918.
- [41] G. S. Brady and H. R. Clauser, *Materials Handbook*, 12th ed., vol. 15, pp. 104-105, 1956.
- [42] W. Goldacker, S. I. Schlachter, B. Obst and M. Eisterer, "In-situ  $MgB_2$  round wires with improved properties," *Supercond. Sci. Technol.*, vol. 17, pp. S490-495, 2004.